

# Composition templating for heterogeneous nucleation of intermetallic compounds

Z. P. Que, Y. P. Zhou, Y. Wang, Z. Fan

BCAST, Brunel University London, Uxbridge, Middlesex, UB8 3PH, UK

## Abstract

Heterogeneous nucleation of intermetallic compounds (IMCs) is inherently more difficult than that of a pure metal or a solid solution. It requires not only the creation of a crystal structure but also the positioning of 2 or more types of elements in the lattice with specified compositions. This makes composition templating a very important approach to nucleation control in addition to structural templating. In this paper we demonstrate composition templating as an approach to enhancing heterogeneous nucleation of IMCs. We found that heterogeneous nucleation of Fe-bearing IMCs in Al-alloys requires an undercooling few tens of K, which is more than an order of magnitude higher than that for solid solutions. Segregation of Fe to the  $TiB_2$  surface (the Fe modified  $TiB_2$ ) can provide composition templating and hence enhance heterogeneous nucleation of  $\alpha-Al_{15}(Fe, Mn)_3Si_2$  resulting in a significant grain refinement

Keywords: heterogeneous nucleation, composition templating, intermetallic compound.

## 1. Introduction

Although heterogeneous nucleation plays a critical role in determining the final solidified microstructure, our current understanding on the subject is rather limited [1]. In recent years there have been a significant amount of effort dedicated to advancing our understanding of heterogeneous nucleation through both theoretical and experimental approaches. Our research showed that heterogeneous nucleation is initiated at temperatures above the liquidus by pronounced atomic ordering in the liquid at the substrate/liquid interface (SuLI) [2]. This phenomenon has been referred as to prenucleation [3]. We found that the degree of prenucleation depends strongly on the lattice misfit between the substrate and the equilibrium solid to be nucleated [3]. At a temperature below the liquidus heterogeneous nucleation occurs by structural templating and proceeds by a layer-by-layer growth mechanism [4]. This suggests that heterogeneous nucleation can be enhanced by reducing the lattice misfit. More importantly, we found that the lattice misfit can be manipulated by interfacial segregation at the SuLI at the prenucleation stage, which can either promote or impede heterogeneous nucleation [5, 6].

Heterogeneous nucleation of intermetallic compounds (IMCs) is much more complicated than that of a pure metal or a solid solution. It requires the creation of not only a crystal structure but a super-structure involving two or more elements. This means that heterogeneous nucleation of IMCs involves both structural templating and compositional templating.

Practically, understanding of heterogeneous nucleation and grain refinement of Fe-bearing IMCs is of great importance. Fe is the most detrimental impurity element in both primary and recycled Al-alloys. It promotes the formation of coarse Fe-bearing IMC platelets which deteriorates mechanical performance of Al-castings. Fundamental understanding of heterogeneous nucleation of Fe-bearing IMCs will lead to the development of effective techniques to refine such IMCs so to mitigate their detrimental effect on mechanical properties.

In this paper we present an overview of our work on composition templating for enhancing heterogeneous nucleation of Fe-bearing IMCs in Al-alloys.

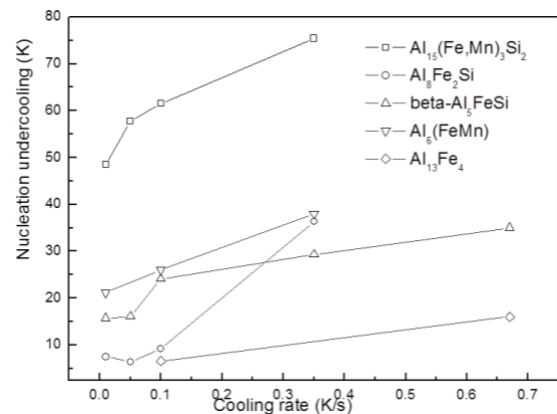


Figure 1: Nucleation undercooling for different types of Fe-bearing IMCs in Al-alloys measured by DSC technique as a function of cooling rate.

## 2. Heterogeneous nucleation and grain refinement of IMCs

To probe into heterogeneous nucleation of IMCs, we measured the nucleation undercooling of different types of Fe-bearing IMCs in Al-alloys by the standard DSC technique. CALPHAD approach was used to select alloy compositions which ensures a particular type of Fe-bearing IMC is the primary phase of suitable volume fraction to facilitate the DSC investigation. Both chemical compositions and resultant microstructures were examined to confirm that the selected samples for DSC study are representative of the bulk alloys. The measured nucleation undercooling for different types of Fe-bearing IMCs are presented in Fig. 1 as a function of cooling rate in the range of industrial relevance.

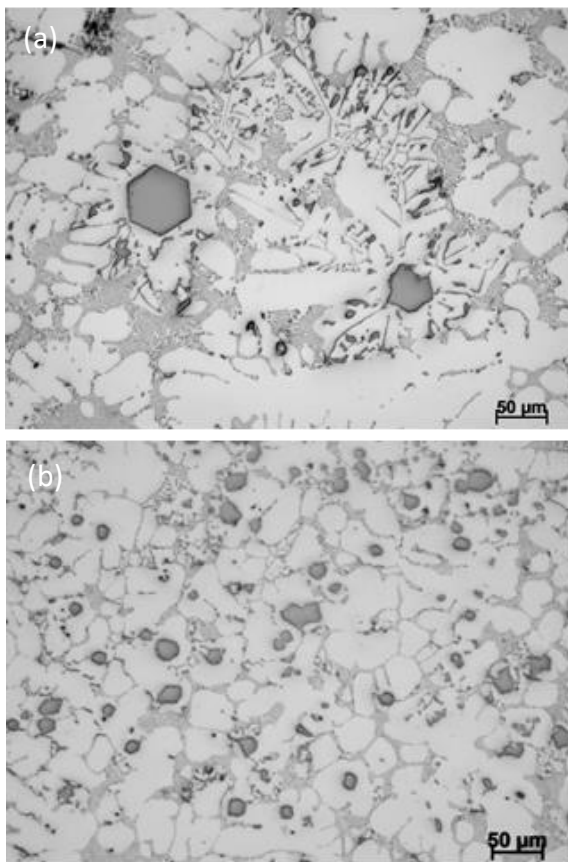


Figure 2: Optical micrographs showing the microstructures of Al-5Mg-2Si-1.1Fe-0.7Mn alloy (a) without and (b) with the addition of Fe-modified TiB<sub>2</sub> particles. The  $\alpha$ -Al<sub>15</sub>(Fe,Mn)<sub>3</sub>Si<sub>2</sub> phase has been significantly grain refined by the addition of the Fe-modified TiB<sub>2</sub> particles.

The results in Fig. 1 released the following facts:

- The nucleation undercooling required for nucleation of IMCs is generally a few tens of K and is more than an order of magnitude higher than that for solid solutions.
- Nucleation undercooling increases with increasing complexity of the IMCs. The more the elements in an IMC, the higher the undercooling.

- Nucleation undercooling increases with increasing cooling rate.

These facts suggest that heterogeneous nucleation of IMCs is more difficult compared with that of simple solid solutions. It requires not only structural templating to create the crystal structure but also chemical compositions and atomic arrangement of the constitute elements within the crystal structure. This makes the supply of the constitute atoms to the SuLI becoming a critical factor for heterogeneous nucleation of IMCs.

Intuitively, one would expect that segregation of the constitute elements at the SuLI would provide the initial supply partially the required constitute elements, and therefore facilitate heterogeneous nucleation of the IMC.

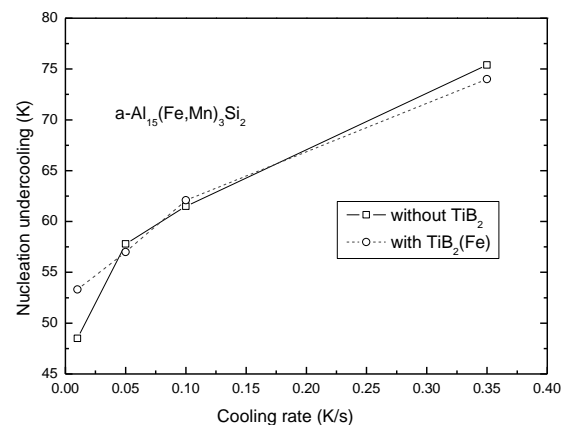


Figure 3: Nucleation undercooling for the  $\alpha$ -Al<sub>15</sub>(Fe,Mn)<sub>3</sub>Si<sub>2</sub> phase during solidification of Al6Si-5Fe-4Mn alloy with and without addition of Fe-modified TiB<sub>2</sub> particles as a function of cooling rate.

Specially designed experiments have been conducted to test this hypothesis. TiB<sub>2</sub> particles were produced through chemical reaction between Ti and B in Al melt at high temperature. The Al melt containing both TiB<sub>2</sub> particles and high Fe content were isothermally held at high temperature for sufficient period of time to allow the segregation of Fe on the TiB<sub>2</sub>/liquid interface through adsorption. The master alloy containing Fe-modified TiB<sub>2</sub> particles were then used to inoculate Al-5Mg-2Si-1Fe-0.7Mn alloy. As shown in Fig. 2, a significant grain refinement of the primary  $\alpha$ -Al<sub>15</sub>(Fe,Mn)<sub>3</sub>Si<sub>2</sub> phase was achieved with such master alloy addition compared with that without the addition of the master alloy.

However, further DSC investigation of the nucleation undercooling revealed that addition of Fe-modified TiB<sub>2</sub> particles did not reduce the nucleation undercooling (Fig. 3) although significant grain refinement was achieved

## 3. Composition templating

High resolution TEM/STEM examination and STEM/superX-EDS analysis were conducted to confirm the nature of interfacial segregation of Fe on the TiB<sub>2</sub> surface. It is confirmed that Fe atoms segregate on both basal and prismatic planes of TiB<sub>2</sub> particles (hexagonal plates) although the segregation on the prismatic plane

appears to be stronger than that on the basal plane (Fig. 4). Similar to many other interfacial segregations by adsorption, Fe segregation on the  $\text{TiB}_2$  surface is a monolayer of Fe-rich atoms. Further investigation is required to establish the exact atomic arrangement in the segregated Fe-rich monolayer.

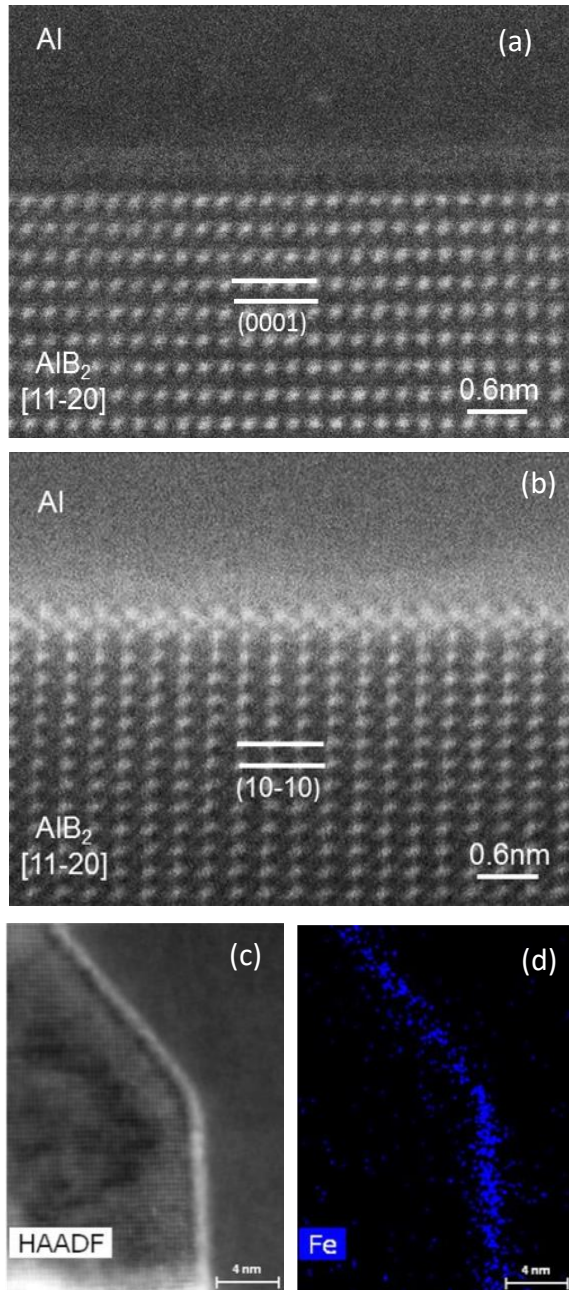
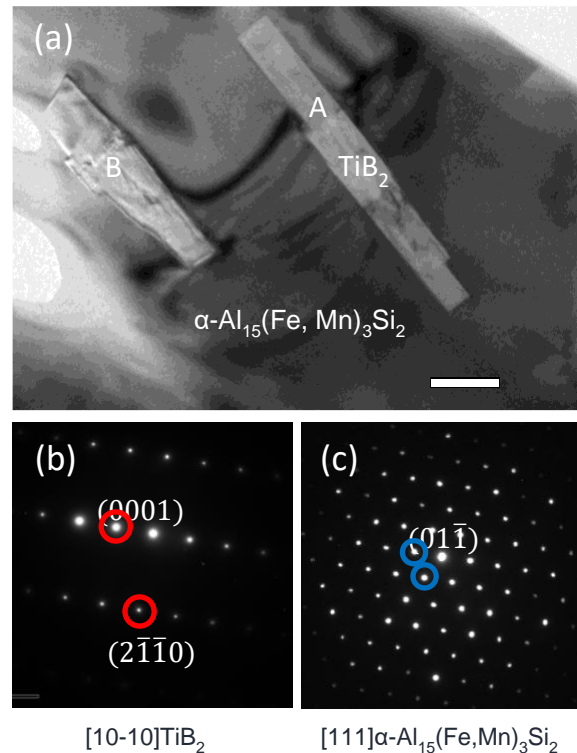


Figure 4: High resolution STEM HAADF images showing segregation of Fe atoms (confirmed by super X-EDS analysis) on (a) prismatic plane and (b) basal plane of  $\text{TiB}_2$ . (c) STEM HAADF image and (d) super X-EDS mapping showing That Fe is enriched on the surface of  $\text{TiB}_2$  particle.

The Fe-modified  $\text{TiB}_2$  particles are much more frequently found within the  $\alpha\text{-Al}_{15}(\text{Fe},\text{Mn})_3\text{Si}_2$  compound than the  $\text{TiB}_2$  particles without Fe- modification. Multiple  $\text{TiB}_2$  particles were observed in a single  $\alpha\text{-Al}_{15}(\text{Fe},\text{Mn})_3\text{Si}_2$

particle. This suggest that Fe-modification has possibly reduced the interfacial energy between  $\text{TiB}_2$  and  $\alpha\text{-Al}_{15}(\text{Fe},\text{Mn})_3\text{Si}_2$  and that between  $\text{TiB}_2$  and liquid Al. This creates a more favourable condition for engulfing  $\text{TiB}_2$  particles into the growing  $\alpha\text{-Al}_{15}(\text{Fe},\text{Mn})_3\text{Si}_2$  compound during solidification. Fig. 5a shows a TEM bright field image  $\alpha\text{-Al}_{15}(\text{Fe},\text{Mn})_3\text{Si}_2$  compound (viewed from the [111] direction) containing 2  $\text{TiB}_2$  particles (Particle "A" was viewed from the [10-10] direction).

Figure 5 (a) TEM bright field image showing the Fe-modified  $\text{TiB}_2$  particles embedded in  $\alpha\text{-Al}_{15}(\text{Fe},\text{Mn})_3\text{Si}_2$  intermetallic compound, (b) and (c) are selected area electron diffraction patterns taken from the boride particle and the intermetallic phase with [10-10] and [111] zone direction, respectively.



Further HRTEM examination showed that only one  $\text{TiB}_2$  particle acted as substrate for heterogeneous nucleation of the  $\alpha\text{-Al}_{15}(\text{Fe},\text{Mn})_3\text{Si}_2$  phase (e.g., particle "A" in Fig. 5a) and other  $\text{TiB}_2$  particles are simply engulfed in the same  $\alpha\text{-Al}_{15}(\text{Fe},\text{Mn})_3\text{Si}_2$  particle during crystal growth (e.g., particle "B" in Fig. 5a). Fig. 6 is a HRTEM image of the interface between  $\text{TiB}_2$  particle (particle "A" in Fig. 5a) and the  $\alpha\text{-Al}_{15}(\text{Fe},\text{Mn})_3\text{Si}_2$  phase. Fast Fourier transformation (FFT) patterns for  $\text{TiB}_2$  (Fig. 5b) and the  $\alpha\text{-Al}_{15}(\text{Fe},\text{Mn})_3\text{Si}_2$  phase (Fig. 5c) reveals a specific orientation relationship (OR):

$$(0001) [10-10]_{\text{TiB}_2} // (01-1) [111]_{\alpha\text{-Al}_{15}(\text{Fe},\text{Mn})_3\text{Si}_2}$$

Carefully controlled tilting experiments during TEM examination have confirmed that the nucleated  $\alpha\text{-Al}_{15}(\text{Fe},\text{Mn})_3\text{Si}_2$  phase on the (0001)  $\text{TiB}_2$  surface is twisted  $4.5^\circ$  along [0001]  $\text{TiB}_2$  axis. This twist suggest that there is a relatively large lattice misfit between Fe-modified  $\text{TiB}_2$  and the  $\alpha\text{-Al}_{15}(\text{Fe},\text{Mn})_3\text{Si}_2$  phase according to the epitaxial nucleation mechanism [3, 4].

$\alpha\text{-Al}_{15}(\text{Fe},\text{Mn})_3\text{Si}_2$  has a complex BCC crystal structure with a lattice parameter of  $12.56\text{\AA}$ , and contains Al, Fe, Si and Mn (Fig. 7a). Al, Fe and Si atoms have specific

positions in the crystal lattice and Mn atoms share some of the lattice positions with Fe atoms.

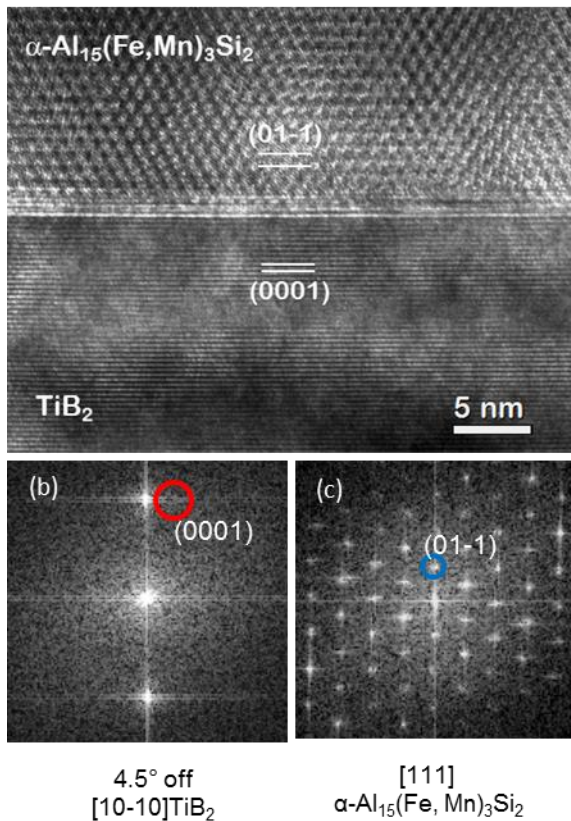


Figure 6: (a) High resolution TEM image showing the interface between  $\text{TiB}_2$  particle and  $\alpha\text{-Al}_{15}(\text{Fe,Mn})_3\text{Si}_2$  phase with  $\text{TiB}_2$  and  $\alpha\text{-Al}_{15}(\text{Fe,Mn})_3\text{Si}_2$  being viewed along  $[10\text{-}10]$  and  $[111]$  ( $4.5^\circ$  deviation), respectively; (b) and (c) are Fast Fourier transformation (FFT) patterns for  $\text{TiB}_2$  and  $\alpha\text{-Al}_{15}(\text{Fe,Mn})_3\text{Si}_2$ , respectively.

The atomic arrangement in  $\{011\}$   $\alpha\text{-Al}_{15}(\text{Fe,Mn})_3\text{Si}_2$  plane is shown in Fig. 7b and is superimposed on the Ti terminated (0001)  $\text{TiB}_2$  surface. A twist of  $4.5^\circ$  of the  $\{011\}$   $\alpha\text{-Al}_{15}(\text{Fe,Mn})_3\text{Si}_2$  plane relative to the (0001)  $\text{TiB}_2$  plane along  $[0001]$   $\text{TiB}_2$  axis (Fig. 7b) showing a better atomic matching than without the twist. The lattice misfit with  $4.5^\circ$  twin is 4.9%, which is relatively large in terms of heterogeneous nucleation. This is in good agreement with our MD simulation of heterogeneous nucleation, which showed that a twist of  $4\text{-}5^\circ$  is required for heterogeneous nucleation with a lattice misfit of 5% [3]. It should be noted that this crystallographic analysis of lattice misfit does not take into consideration of the Fe segregation on the  $\text{TiB}_2$  surface, which is expected to modify the lattice misfit in practical cases.

## 4. Summary

- DSC technique was used to measure the nucleation undercooling of various Fe-bearing IMCs. We found that the undercoolings for nucleation of such IMCs are a few tens of K and increase with the increase of

complexity of the IMC; the more elements in the compound, the higher the undercooling required.

- Segregation of Fe on the  $\text{TiB}_2$  surface provides composition templating and hence enhances heterogeneous nucleation of the  $\alpha\text{-Al}_{15}(\text{Fe,Mn})_3\text{Si}_2$  phase resulting in a significant refinement of  $\alpha\text{-Al}_{15}(\text{Fe,Mn})_3\text{Si}_2$ .
- Structural templating of  $\alpha\text{-Al}_{15}(\text{Fe,Mn})_3\text{Si}_2$  by (0001)  $\text{TiB}_2$  surface leads to a  $4.5^\circ$  twist of the  $\alpha\text{-Al}_{15}(\text{Fe,Mn})_3\text{Si}_2$  crystal along the  $[10\text{-}10]$   $\text{TiB}_2$  axis due to the large misfit.

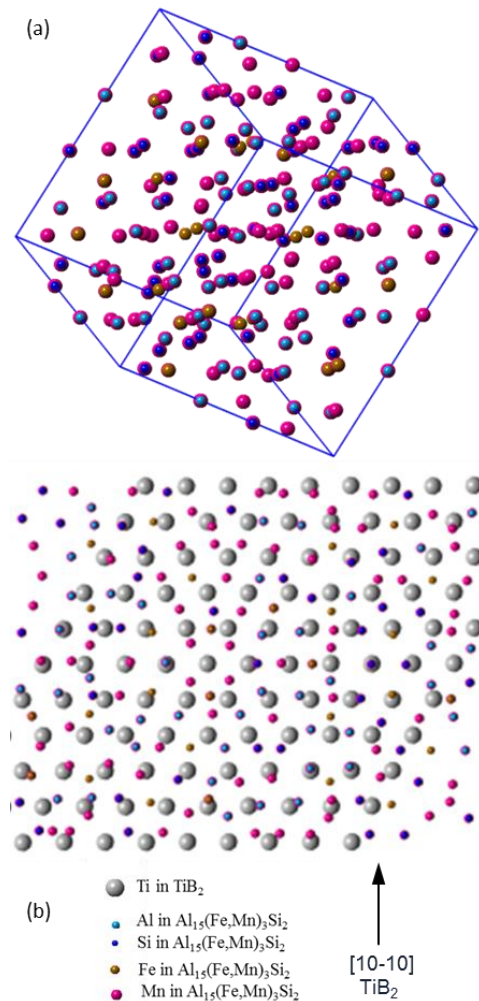


Figure 7: (a) Atomic arrangement in the BCC  $\alpha\text{-Al}_{15}(\text{Fe,Mn})_3\text{Si}_2$  compound, and (b) atomic matching at the  $\text{TiB}_2/\alpha\text{-Al}_{15}(\text{Fe,Mn})_3\text{Si}_2$  interface. The  $\{110\}$   $\alpha\text{-Al}_{15}(\text{Fe,Mn})_3\text{Si}_2$  plane has been twisted  $4.5^\circ$  along the  $[10\text{-}10]$   $\text{TiB}_2$  axis.

## Acknowledgements

EPSRC is gratefully acknowledged for providing financial support under Grant EP/H026177/1.

## References

1. K.F. Kelton *et al.*, *Nucleation in Condensed Matter: Applications in Materials and Biology*, Amsterdam, 2010.
2. H. Men *et al.*, *Comp. Mater. Sci.*, 2014, 85: 1.
3. H. Men *et al.*, *in this Proceedings*, 2017.

4. Z. Fan, *Metall. Mater. Trans. A*, 2013, **44**: 1409.
5. Z. Fan *et al.*, *Acta Mater.*, 2015, **84**: 292.
6. Y. Wang *et al.*, *in this Proceedings*, 2017.